Dynamics of Circular Periodic Structures

THOMAS J. McDANIEL*
University of Dayton, Dayton, Ohio

The frequency response matrix is determined for a periodically supported, periodically damped, closed circular beam structure which is an approximate model of a skin-stringer aircraft fuselage structure. The analytical technique which is developed depends on the periodic nature of the structure to simplify the analysis. The analysis is a complementary approach to the transfer matrix method for determining frequency response. One purpose of the analysis is to circumvent the numerical and/or computer storage difficulties commonly found in computing the frequency response for typical aircraft fuselage structure from a transfer matrix analysis. Numerical difficulty is avoided by using the properties of the transfer matrix for one periodic unit and a consequence of the Cayley-Hamilton theorem to obtain an analytical solution for the frequency response matrix. The second purpose of the analysis is to investigate the spatial decay of response from a point or region of the structure which is being excited. This spatial decay isolates the response to a region of structure near the excitation and reduces the over-all dynamic stress level of the structure for a general excitation. Three damping devices that utilize a viscoelastic link to produce spatial decay are evaluated. Several numerical examples are shown.

Introduction

MANY practical structures, including aircraft structures, are assembled in a series of connected identical units. These structures are known as periodic structures. The subject of this analysis is the forced response of the periodic structure of Fig. 1, which is a complete circular beam supported by a number of identical, equally-spaced elastic supports. The structure is an approximate model for an aircraft fuselage where response midway between the circular frames is of interest. In addition to the basic structure, various high damping devices to control the response can be added so that the resulting structure remains periodic.

It is the spatial repetition of a periodic structure (Fig. 1) which makes its analysis in simple form possible. Analyses of the free vibration of one-dimensional, periodic beam structures are carried out in Refs. 1 and 2. References 3 and 4 present the free vibration analysis of two-dimensional structures, such as a periodic beam grillage and a flat periodic skin-stringer structure. Analyses of the free vibration of closed periodic structures are presented in Ref. 5 for a ring-stiffened, periodic cylinder, and in Refs. 6 and 7 for a periodic skin-stringer structure between adjacent circular frames.

While the previous analyses were directed toward obtaining free vibration information concerning periodic structures, a more recent analysis (Ref. 8) discusses the forced vibration of periodic Bernoulli-Euler flat beam structures. This analysis takes advantage of recent advances in the field of transfer matrix analysis (Refs. 9 and 10) to obtain a matrix formulation of the analysis of flat skin-stringer aircraft structure. The advantages of the transfer matrix analyses of forced response (Ref. 10), such as accounting for a complicated structural configuration which includes damping devices, accounting for random excitation, and permitting a straightforward application of boundary conditions at the ends of the structure, were applied to the periodic structural analysis of Ref. 8. The purpose of the periodic structural analysis was to circumvent numerical difficulties found in Ref. 10 when the determination of the forced response of a large number of spans of typical flat aircraft structure was required. These difficulties are presented in detail in Ref. 8.

Received February 17, 1970; revision received June 22, 1970. This work was sponsored by the U. S. Air Force under Contract No. F33615-67-C-1187.

* Research Engineer, Research Institute. Member AIAA.

Since a large number of periodic units (50 to 200 panels and stringers) are common in aircraft fuselage construction, and since the stringers are quite stiff in comparison to the skin, numerical difficulties similar to those of the flat structure analysis exist when computing the forced response of the curved fuselage. Since the approximate model used in the present study (Fig. 1) contains the essential characteristics of a typical periodic fuselage structure, it is believed that a successful method for overcoming the numerical difficulty involved in computing the forced response of this model can be applied to a more complicated shell-stringer model of fuselage structure. The capability to perform these computations is one of the main reasons for conducting the analytical development included herein.

This analysis also enables an investigation of the spatial decay of response of the curved structure on either side of a region or point of excitation. A study of spatial decay in flat

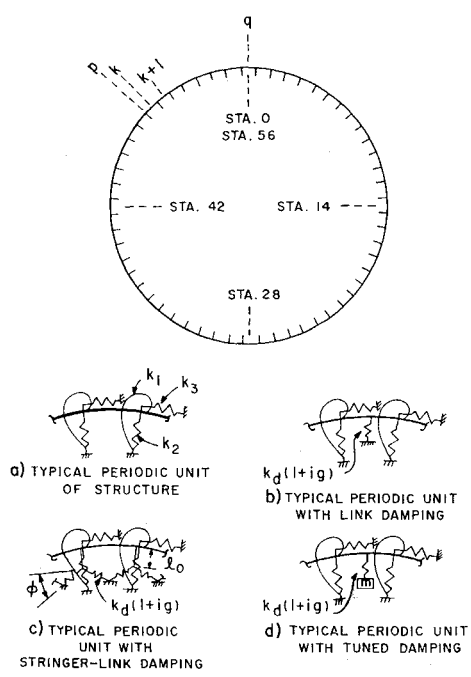

Fig. 1 Periodic closed circular structure.

beam structure can be found in Ref. 15. Such a decay of the response indicates that the response is isolated about the source of excitation and should reduce the over-all dynamic stresses in the structure. The effectiveness of a given damping device can be evaluated by observing whether or not the damping device can produce a spatial decay of response, and by observing the rate of that spatial decay. Thus, the evaluation of specialized damping devices such as viscoelastic links attached between sections of a periodic structure, and tuned dampers attached at various points on the structure, constitutes a second reason for conducting the analysis described in this paper.

The following discussion of the forced response of periodic closed structure will center on the determination of frequency response functions. These functions are important in the analysis of both deterministic and random vibration response, as well as in the study of the rate of spatial decay of response produced by different damping devices on a closed periodic structure.

Conventional Transfer Matrix Analysis of a Closed Circular Structure

Consider the harmonic motion of a point q on the closed circular structure of Fig. 1. Noting that the radial and circumferential responses are of interest, the state of motion at a given point on the structure can be described by a vector

$$\mathbf{Z}e^{i\omega t} = \{u,\delta,\varphi,M,V,N\}e^{i\omega t} \tag{1}$$

where $\{\ \}$ denotes a column vector. The column vector $\mathbf{Z}$ is called a state vector and, reading from top to bottom in the previous matrix, its components are the complex amplitudes of circumferential displacement, radial displacement, rotation of the cross section, moment, shear, and circumferential force. The common factor $e^{i\omega t}$ is omitted in the following discussion of the analysis. If excitation is external to the interval between two arbitrary stations q and r on the structure, the state vectors at these two points are related by

$$\mathbf{Z}_r = \mathbf{T}_{r\leftarrow q}\mathbf{Z}_q \tag{2}$$

where $\mathbf{T}_{r\leftarrow q}$ is the transfer matrix associated with the structural elements connecting points q and r. In this analysis, $\mathbf{T}_{r\leftarrow q}$ is a 6×6 complex-valued matrix. When excitation occurs in the interval between stations q and r, at station p, for example, the state vectors at q and r are related by

$$\mathbf{Z}_r = \mathbf{T}_{r\leftarrow q}\mathbf{Z}_q + \mathbf{T}_{r\leftarrow p}\mathbf{Y}_p \tag{3}$$

where $\mathbf{Y}_p$ is the input at station p. The vector $\mathbf{Y}_p$ contains the amplitudes of the harmonic excitations at point p, which produce the steady-state harmonic responses at points q and r.

$$\mathbf{Y}_p e^{i\omega t} = \{0,0,0,\ -Q,P,\ -R\}_p e^{i\omega t} \tag{4}$$

The quantities Q, P, and R are, respectively, the amplitudes of the moment, shear, and circumferential force excitations which are considered.

The conventional transfer matrix analysis of the closed circular structure can now be completed. Point q is chosen as a reference point on the structure. If the state vector $\mathbf{Z}_q$ at q is transferred through one circumference of the closed circular structure, the resulting state vector $\mathbf{Z}_{q'}$ is obtained. For continuity

$$\mathbf{Z}_{q'} = \mathbf{Z}_q \tag{5}$$

Equation (3) in this case becomes

$$\mathbf{Z}_q = \mathbf{T}_{q'\leftarrow q}\mathbf{Z}_q + \mathbf{T}_{q'\leftarrow p}\mathbf{Y}_p \tag{6}$$

The response at q because of the excitation at p can be obtained from Eq. (6) as

$$\mathbf{Z}_q = -[\mathbf{T}_{q'\leftarrow q} - \mathbf{I}]^{-1}\mathbf{T}_{q'\leftarrow p}\mathbf{Y}_p \tag{7}$$

where $\mathbf{I}$ is the identity matrix. The matrix which relates the harmonic excitation of frequency ω at p to the steady-state response at q, is known as the frequency response matrix and is denoted by $\mathbf{H}_{qp}(\omega)$ and is given by

$$\mathbf{H}_{qp}(\omega) = -[\mathbf{T}_{q'\leftarrow q} - \mathbf{I}]^{-1}\mathbf{T}_{q'\leftarrow p} \tag{8}$$

If the closed circular structure is composed of a large number of spans, and/or is supported by elastic supports which are quite stiff in comparison to the beam stiffness, numerical difficulty will result from computing Eq. (8) by direct numerical operations. See Ref. 8 for additional discussion of those cases where numerical difficulty can result in the transfer matrix method of computing $\mathbf{H}_{qp}(\omega)$ for flat structure. It is sufficient to note that for both the flat and closed circular structures, numerical difficulties are particularly severe near the maximum response of the structure where computational accuracy is desired.

A Complementary Transfer Matrix Approach for Periodic Closed Circular Structure

Since numerical difficulty will result from the use of a conventional transfer matrix analysis of a practical fuselage structure, a complementary approach was developed for the case of periodic structure. Referring to the approximate model of periodic fuselage structure in Fig. 1, adjacent periodic stations which separate the periodic units of the model are labeled by integer values of 0, 1, 2, ..., N, where N is the total number of spans or units of the closed structure. If excitation is external to a unit of the structure, the transfer matrix relationship between periodic stations n and $n + 1$ of the structure is

$$\mathbf{Z}_{n+1} = \mathbf{T}\mathbf{Z}_n \tag{9}$$

For the periodic structure, Eq. (7) can be rewritten as

$$\mathbf{Z}_q = -[\mathbf{T}^N - \mathbf{I}]^{-1}\mathbf{T}^{N-k}\mathbf{T}_{k\leftarrow p}\mathbf{Y}_p \tag{10}$$

Since the response $\mathbf{Z}_q$ is of interest, station q has been chosen as a periodic station on the structure. In Eq. (10), $\mathbf{T}^N$ denotes a transfer over one circumference of the closed structure, and $\mathbf{T}^{N-k}\mathbf{T}_{k\leftarrow p}$ is a transfer of the excitation from station p to station q, which includes a transfer over a portion of one unit of structure between point p and the kth periodic station, and finally over $N - k$ units of periodic structure. The points p, k, and q are illustrated in Fig. 1.

The advantage of Eq. (10) is that the properties of the transfer matrix $\mathbf{T}$ can be used to reduce the numerical difficulty in computing $g(\mathbf{T})$ where

$$g(\mathbf{T}) = -[\mathbf{T}^N - \mathbf{I}]^{-1}\mathbf{T}^{N-k} \tag{11}$$

Note that $g(\mathbf{T})$ is the frequency response matrix, i.e.,

$$\mathbf{H}_{qp}(\omega) = g(\mathbf{T}) \tag{12}$$

when both q and p are periodic stations of the structure.

To compute $\mathbf{H}_{qp}(\omega)$ accurately, the properties of $\mathbf{T}$ as discussed in Appendix 1 of Ref. 8 are employed. Since $\mathbf{T}$ is a transfer matrix, the inverse of $\mathbf{T}$ exists because

$$|\mathbf{T}| = |\mathbf{T}^{-1}| = 1 \tag{13}$$

where $|\ |$ denotes the determinant of a matrix. Thus, $g(\mathbf{T})$ can be expressed in the form

$$g(\mathbf{T}) = \sum_{j=1}^{3} a_j \frac{(\mathbf{T}^j + \mathbf{T}^{-j})}{2} + b_j \frac{(\mathbf{T}^j - \mathbf{T}^{-j})}{2} \tag{14}$$

as a consequence of the Cayley-Hamilton theorem. The coefficients a_j and b_j, which are functions of N and k, are computed from the simultaneous equations obtained by substituting the distinct eigenvalues of $\mathbf{T}$ (i.e., λ_j for $1 \leq j \leq 6$) for matrix $\mathbf{T}$ in Eq. (14). To obtain the eigenvalues of matrix $\mathbf{T}$, one computes $|T - \lambda I| = 0$. The resulting char-

acteristic equation for **T** is given by

$$\lambda^6 - 2K_1\lambda^5 + 2K_2\lambda^4 - 2K_3\lambda^3 + 2K_2\lambda^2 - 2K_1\lambda + 1 = 0 \quad (15)$$

The K_j's, which are the sums of the principal minors of **T**, are computed as

$$2K_1 = \sum_{i=1}^{6} t_{ii}$$

$$2K_2 = \sum_{j=1}^{6}\sum_{i=1}^{6} t_{ii}t_{jj} - t_{ij}t_{ji} \text{ for } i > j \quad (16)$$

$$2K_3 = \sum_{i=1}^{6}\sum_{j=1}^{6}\sum_{k=1}^{6} t_{ii}t_{jj}t_{kk} + t_{ij}t_{jk}t_{ki} + t_{ji}t_{kj}t_{ik} - t_{ik}t_{jj}t_{ki} - t_{ij}t_{ji}t_{kk} - t_{jk}t_{kj}t_{ii} \text{ for } i > j > k$$

The form of the eigenvalues obtained from Eq. (15) must be $\lambda = e^{\pm i\theta}$. The characteristic equation can be reduced by direct substitution to a cubic equation in $\cos\theta$. The roots of the characteristic equation are of the form

$$\cos\theta_j = x_j + iy_j = Z_j, j = 1, 2, 3 \quad (17)$$

where $i = (-1)^{1/2}$. The right side of Eq. (17) is generally complex valued; thus, the θ'_js are obtained from

$$\theta_j = -i \ln[Z_j + (Z_j^2 - 1)^{1/2}] \quad (18)$$

The a_j and b_j's of Eq. (14) can be obtained by inserting the eigenvalues of **T** for matrix **T**, by performing the addition, and by subtracting the two equations resulting from each conjugate pair of eigenvalues. These simultaneous equations for the case where θ'_ls are distinct are

$$\frac{\cos(N-k)\theta_l + \cos k\theta_l}{2(1 - \cos N\theta_l)} = \sum_{j=1}^{3} a_j \cos j\theta_l$$

$$\frac{\sin(N-k)\theta_l + \sin k\theta}{2(1 - \cos N\theta_l)} = \sum_{j=1}^{3} b_j \sin j\theta_l \; l = 1,2,3 \quad (19)$$

Cases where two and possibly three of the θ_l's are equal can occur, but this implies a definite relationship between the structural parameters and the frequency of excitation. There can at most be a discrete number of these frequencies over a given range of harmonic excitation.

Additive Structural Damping

Three procedures for introducing damping by the use of a viscoelastic link are considered for this analysis. Of particular interest is the capability of the link to control the large responses of the structural model and to isolate the excitation by causing a spatial decay of response. In Fig. 1b, damping is obtained by attaching one end of a viscoelastic link to the midpoint of each beam segment and by attaching the other end radially to a rigid substructure. A second use of the viscoelastic link to obtain damping is shown in Fig. 1c for a typical unit of structure. In the actual structure, the viscoelastic link would be attached to adjacent stringers and anchored midway between the stringers to a substructure. In the beam model, the stringer attachment of the viscoelastic link is simulated by a rigid, massless member having a length l_0. This member couples the viscoelastic link with the motion of the beam by adding to the forces exerted by each elastic support of the beam model. This configuration is denoted as stringer-link damping. An experimental study of a similar stringer-link damping configuration has been considered in Ref. 11; however, in this Reference, the links were not anchored to the substructure between stringers. The third use of the viscoelastic link as a damping device (Fig. 1d) is a viscoelastic link with a suspended mass (a tuned damper). Reference 11 has demonstrated experimentally the potential of the tuned damper in controlling specific responses of aerospace structures.

The transfer matrices for a segment of a circular beam, the elastic support, and the various point damping devices are thus needed to carry out the numerical study. These matrices are listed in Appendix. A brief derivation of the transfer matrix for the curved beam segment is presented in Appendix since it was not found in the literature, although some limiting cases of this result were reported in Ref. 13.

Numerical Examples

Typical frequency response functions are generated for the closed periodic structure of Fig. 1. Since it is desired to approximate typical aircraft fuselage structure, the properties of the periodic fuselage structure considered in Ref. 6 are duplicated in the present analysis. The total number of spans of the model is 56, and the properties of the circular beam between two adjacent supports in the model are h: thickness: 0.04 in.; E: elastic modulus: 10.5×10^6 psi; l: span length: 8.2 in.; R: radius of beam: 73.084 in.; μ: mass density per unit length of beam: 1.046×10^{-5} lb-sec^2/in.^{3} For each elastic support, the properties are k_1: rotational spring stiffness: 180 in.-lb/rad; k_2: radial deflection spring stiffness: 1100 lb/in.; k_3: circumferential spring stiffness: 750 lb/in.

All of the following results are computed for a shear-type excitation at station 0, which is located at midspan of a typical unit of the periodic structure. A unit shear excitation requires that $P = 1.0$, $Q = 0.0$, and $R = 0.0$ in Eq. (4). The radial deflection frequency response produced by this excitation is illustrated as a function of forcing frequency and distance from the point of excitation (station 0) in the following examples.

Undamped Radial Deflection Response

To obtain some comparison of the beam model analysis with the fuselage analysis of Ref. 6, the undamped response of the beam model was computed first. The natural frequency of the beam model was found by forcing the model at a frequency for which the elements of the frequency response matrix (except for nodal responses) are unbounded. Careful estimation of the spring constants for the elastic supports of the beam model resulted in good agreement (within 4%) of the first natural frequency of the model (636.303 rad/sec) with the first natural frequency of the fuselage structure analyzed by Ref. 6.

The radial response of the entire 56-span model was calculated at a forcing frequency within 0.001 rad/sec of the first natural frequency of the model. This response was produced by the shear-type excitation and was normalized such that a unit amplitude of response was maintained at the point of excitation. Figure 2 illustrates, as expected, that near a natural frequency the entire structure responds to the ex-

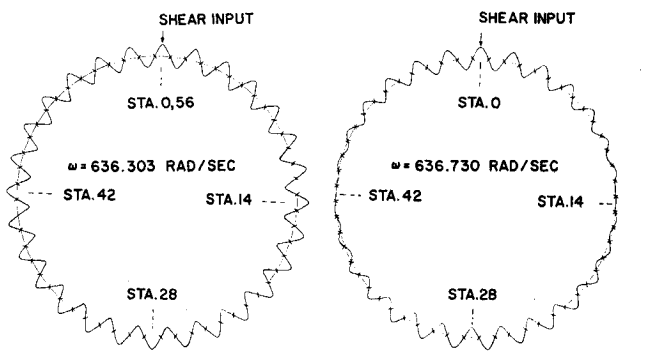

Fig. 2 Radial deflection response of undamped periodic structure with shear excitation at station 0.

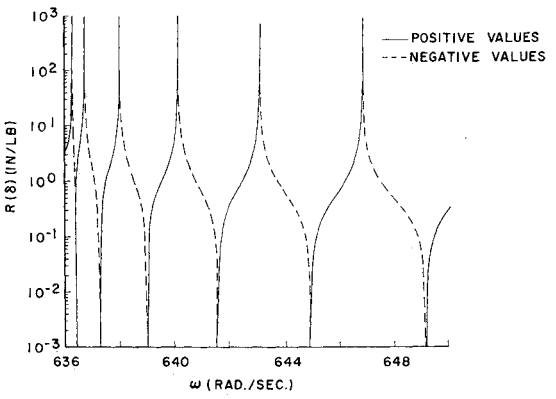

Fig. 3 Radial deflection response vs frequency of undamped periodic structure.

citation in the absence of damping. This deflection shape is the first normalized mode of vibration of the structural model, since it is independent of the source of the excitation. The radial deflection of the model in this mode agrees qualitatively with the assumed mode used by Ref. 6 for calculating the natural frequency of the periodic fuselage discussed previously. Figure 2 further illustrates the radial deflection response for a forcing frequency of 636.730 rad/sec. Note that only symmetric modes are obtainable from the symmetrically applied excitation. Close spacing of the frequencies of the first modes of the model was anticipated from a peak in the power spectral density plot of strain measurements near these frequencies in the actual fuselage structure which the beam model approximates.

The distribution of natural frequencies of the model is further illustrated by the unbounded deflection responses of the structural model as a function of forcing frequency shown in Fig. 3. Only the real part of the deflection response $R(\delta)$ at station 0 is shown, since the imaginary part of the frequency response is zero in the absence of damping.

Frequency Response of the Damped Structure

The effect of periodically-added damping devices on the radial deflection frequency response of the beam model is of particular interest in this analysis. In contrast to the undamped structure, the damped structure has a frequency response which is complex valued, and is defined by its real and imaginary components or equivalently by its amplitude and phase angle. In order to make comparisons of the various damping devices, a unit amplitude shear at station 0 will again be used to excite the structural model in all of the following examples.

Since the damping devices are attached at essentially one point within each periodic unit of the beam, this effect must be converted into an equivalent line effect across the width of the beam. Thus, if a link having a complex stiffness β lb/in. is attached to a beam structure, its effect per unit width of the beam is $k = \beta/l^*$, where k is the complex stiffness of lb/in. per unit width, and l^* is the width of the beam, which may range from 10 in. to 30 in. for the simulation of fuselage structure afforded by the present model.

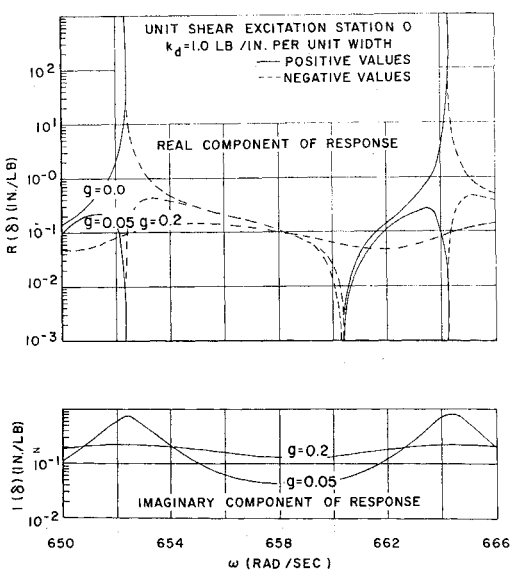

Fig. 4 Components of radial deflection response vs frequency for periodic structure with link damping.

Link Damping

The first type of damping device to be considered is the viscoelastic link damper which is attached on one end at midspan of each periodic unit of the structural model and at the other end to a rigid substructure as shown by Fig. 1b. The complex stiffness of the link per width of the beam is represented by $k = k_d(1 + ig)$, where k_d and g are normally dependent on frequency and are assumed to be constants for the frequency range considered. For the following computations, $k_d = p$ lb/in. per unit width was selected. Three values of g, namely $g = 0.0$, $g = 0.5$, and $g = 0.2$, were used to show the effect of increasing damping on the real and imaginary parts of the radial frequency response, over a frequency range which contains a typical maximum response of the structure. Figure 4 contains an overlay of the real part of these radial deflection responses $R(\delta)$ at station 0 vs forcing frequency. Figure 4 further contains an overlay of the imaginary part $I(\delta)$ of these frequency responses. This figure shows the rapid changes of phase which can occur as a function of forcing frequency in a lightly damped structure.

A significant measure of the effectiveness of any damping device is its ability to control large amplitude responses over a wide frequency range. To illustrate the effectiveness of the link in controlling the radial deflection response, the model was excited by the unit shear excitation at station 0 over a frequency range of excitation extending from below the structure's first frequency response over a 400 rad/sec range. A link stiffness of $k_d = 1$ lb/in. per unit width and values of $g = 0.2$ and $g = 0.5$ are used in the calculations. An overlay of the magnitude of the radial response $|\delta|$ at stations 0, 3, and 7 for the two values of g is presented in Fig. 5. Note that the peaks of response are attenuated, but the minimums of response are increased when the damping is increased from $g = 0.2$ to $g = 0.5$.

The effectiveness of the viscoelastic link damper in producing a spatial decay of response from the source of excitation was next investigated. Since the peak responses of a structure are to be reduced with specialized damping attachments, only the envelopes of the peaks of response were

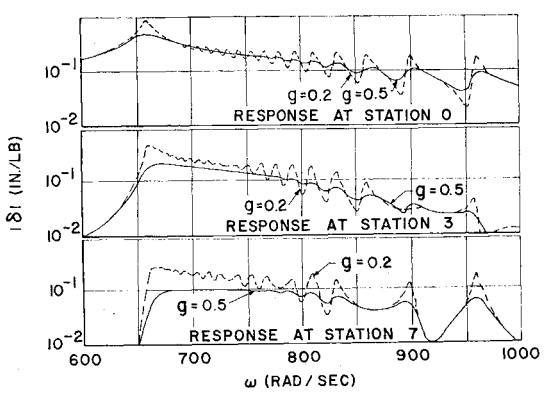

Fig. 5 Absolute value of radial deflection response vs frequency of periodic structure with link damping.

compared in order to evaluate the link damper. No other damping from the structure or the surroundings was considered. In Fig. 5, the envelopes of the deflection response at Stations 0, 3, and 7 produced by the unit shear excitation could be drawn. Note that for $g = 0.2$, Fig. 5 shows a spatial decay of the envelope of the response for 600 rad/sec $\leq \omega \leq$ 870 rad/sec, except near $\omega = 750$ rad/sec and $\omega = 815$ rad/sec where equal responses occur at stations 3 and 7. For $\omega > 870$ rad/sec, a spatial decay of response does not occur since a nodal point of the radial response occurs at some link attachment points. The energy dissipated by those links must now be dissipated by links further from the excitation. Spatial decay of response is more evident as g is increased to 0.5 for the lower frequencies of excitation.

Tuned Damper

A tuned damper element illustrated by Fig. 1d was used instead of the link damper at the center of each span of the model. To illustrate the nature of the spatial decay of response produced by the tuned damper, the envelope of the radial deflection response was plotted over the entire structural model at the frequency of its first maximum of response. Figure 6 shows this envelope of the response which occurs over one cycle of the excitation, irrespective of the phase differences which exist between response at different locations on the structure. This response should be compared to Fig. 2, which is the deflection response over the entire structure near the first maximum response of the undamped structure. Next, the peak envelope of the radial deflection response $|\delta|_p$ was plotted for $k = 1.0$ lb/in. per unit width, $g = 0.2$ for $\omega_T = (k_d/m)^{1/2} = 750$ rad/sec and $\omega_T = 1000$ rad/sec, and these curves are shown in Fig. 7. This plot illustrates the effect of ω_T, the tuned frequency of the damper, on the deflection response at various stations.

Stringer-Link Damper

As a final illustration, the stringer-link damping of Fig. 1c was attached to the model at each support. Figure 8 shows an envelope of the peak radial response $|\delta|_p$ at station 0, 3, and 7 for a viscoelastic link with $k_d = 50$ lb/in. per unit width, and $g = 0.2$. The link was attached such that $l_0 = 1.25$ in. and $\phi = \pi/6$ rad in Fig. 1c. Lower values of k_d were also considered but were not particularly effective in reducing response of the structure.

Discussion

The preceding numerical examples illustrate three uses of the viscoelastic link to produce damping in the beam structure. The envelope of the response under the point of excitation (station 0) was found to be an upper bound in all cases to the response at other periodic stations on the structure. Spatial decay of response was not obtained over the entire frequency range of excitation for any of the methods of introducing damping. The link damper and the stringer-link damper were effective in producing spatial decay of response at the lower frequencies of excitation, since large deflection responses and large rotations of the elastic supports are experienced at the points of damper application. Since the response characteristics of the beam structure change with

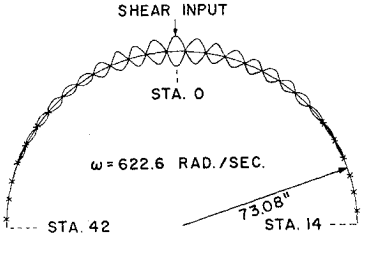

Fig. 6 Envelope of radial deflection response of periodic structure with tuned dampers.

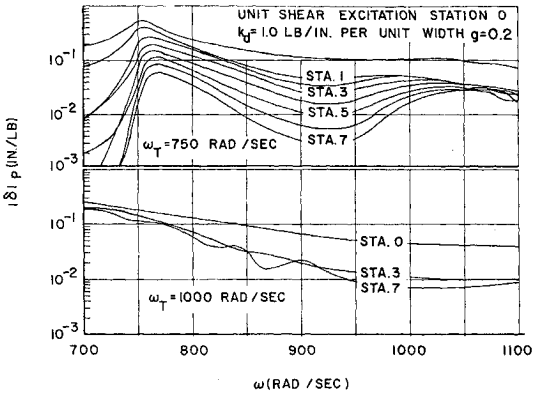

Fig. 7 Envelope of radial peak deflection response vs frequency of periodic structure with tuned damping.

frequency, these two means of introducing damping do not produce a strict spatial decay of response at higher frequencies. The capability of the tuned damper to produce a spatial decay of response in different frequency ranges of excitation by adjusting the tuning of the damper should be noted. Though not illustrated by the numerical results, mass loading from the tuned damper can alter the frequency response of the original structure when the mass of the damper is increased significantly.

The success of the numerical analysis of this approximate model for a typical fuselage structure (one having relatively stiff elastic supports and a large number of spans) depends upon careful numerical manipulations of Eqs. (18) and (19). First, it is necessary to obtain accurate values of θ_j. For cases where the absolute value of Z_j in Eq. (17) is large, Eq. (18) for computing θ_j should be written in the form

$$\theta_j = \theta_{j1} + i\theta_{j2} = -i\ln\{Z_j[1 + (1 - 1/Z_j^2)^{1/2}]\}$$

and a series expansion of the square-root term should be used. Secondly, for the complex θ_j, Eq. (19) contains terms such as $\cosh N\theta_{j2} \cos N\theta_{j1}$, $\sinh N\theta_{j2} \cos N\theta_{j1}$, etc. When $N\theta_{j2}$ is large, terms on the left hand side of Eq. (19) will be obtained from small differences of large numbers. Numerical inaccuracy can be avoided by noting for large $N\theta_{j2}$ that $\cosh N\theta_{j2} \cong e^{N\theta_{j2}}/2$ and that $\sinh N\theta_{j2} \cong e^{N|\theta_{j2}|}/2 \operatorname{sgn}(\theta_{j2})$. $\operatorname{sgn}(\theta_{j2})$ denotes the sign of θ_{j2}. Since computer space is not a problem with the present analysis, double precision computations are possible and desirable.

For the numerical results generated for the damped structure, no frequencies of excitation were found for which two values of $\cos\theta_j$ were identical. The eigenvalues of the transfer matrix are thus distinct and the need for an alternate formulation of Eq. (19) to cover the case of repeated eigenvalues does not appear necessary.

Concluding Remarks

The periodically supported, periodically damped, closed circular beam discussed in this paper may be considered as an

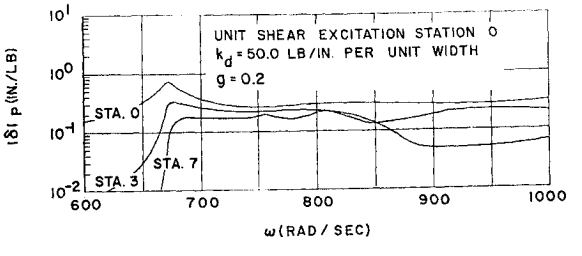

Fig. 8 Envelope of radial peak deflection response vs frequency of periodic structure with stringer-link damping.

approximate model for the skin-stringer periodic aircraft fuselage. By taking advantage of the periodic nature of the beam structure, numerical difficulties and/or computer storage difficulties which one finds in computing the frequency response by an ordinary transfer matrix can be circumvented. The extension of this analysis to the two-dimensional fuselage structure between two circular frames is more complicated due to the increase from a 6×6 transfer matrix for the beam structure to an 8×8 transfer matrix for the fuselage structure. This larger transfer matrix is possible to form (see Ref. 13) when the separation of spatial variables solution is admissible. The capability to compute the frequency response of the closed circular beam having typical aircraft geometry and stiffness indicates that the extension of the type of analysis presented herein to fuselage structure should be successful. Numerical stability of the analysis can be attributed to the use of a consequence of the Cayley-Hamilton theorem which permits the use of an analytical solution for the frequency response matrix and consequently, algebraic manipulation of that matrix for critical numerical operations in the analysis. Furthermore, the inversion of a large structural matrix is not necessary in the present analysis.

With the present technique for computing frequency response, the spatial distribution of response was investigated for three means of introducing damping attached at periodic intervals to the beam structure. A spatial decay of response on either side of the point of excitation indicates that the response of the structure is essentially isolated to a region near the excitation. For a general time and space variation of the excitation, this spatial decay of the frequency response should result in the reduction of the over-all dynamic stresses in such a structure. The effectiveness of damping devices can be evaluated by determining whether or not they can produce a spatial decay of response and by noting the rate of that spatial decay. For the periodically-added damping devices considered, a spatial decay of response was found only over a portion of the frequency range of excitation. This result indicates the necessity of carefully choosing a damping device that will be effective in reducing the stresses of an existing structure over all parts of a specified frequency range.

The advantage of this present analysis in comparison to the normal mode method is evident when the number of closely-spaced modes for the beam structure is considered. Furthermore, the frequency response matrix in this analysis obtains stresses, as well as deflections, directly. The analysis provides the necessary technique for obtaining the damped stress or deflection response of the periodic structure to deterministic or random excitation.

Appendix: Transfer Matrices for Circular Structure

The transfer matrix for a segment of circular beam undergoing harmonic motion can be obtained by solving the matrix differential equation

$$d\mathbf{Z}/ds = \mathbf{AZ} \tag{A1}$$

where the elements of the state vector $\mathbf{Z}$ are defined in the main text [Eq. (1)]. Matrix $\mathbf{A}$ is given in Ref. 9 to be

$$\mathbf{A} = \begin{bmatrix} 0 & -1/R & 0 & 0 & 0 & 1/EA \\ 1/R & 0 & 1 & 0 & 0 & 0 \\ 0 & 0 & 0 & 1/EI & 0 & 0 \\ 0 & 0 & 0 & 0 & 1 & 0 \\ 0 & \mu\omega^2 & 0 & 0 & 0 & -1/R \\ -\mu\omega^2 & 0 & 0 & 0 & 1/R & 0 \end{bmatrix} \tag{A2}$$

R = radius of beam
EI = beam bending stiffness
l = span length of beam
EA = circumferential stiffness
μ = mass per unit length
ω = frequency of vibration

The solution to this matrix differential equation is

$$\mathbf{Z}_{(l)} = \mathbf{F}_{(l)}\mathbf{Z}_{(0)} \text{ where } \mathbf{F}_{(l)} = e^{\mathbf{A}l} \tag{A3}$$

is the transfer matrix for a segment of beam of length l. By use of the Cayley-Hamilton theorem,

$$e^{\mathbf{A}l} = \sum_{j=0}^{5} a_j(l)\mathbf{A}^j \tag{A4}$$

To evaluate the $a_j(l)$'s, one substitutes for matrix $\mathbf{A}$ in Eq. (A4) the eigenvalues of $\mathbf{A}$. Then, from the characteristic equation for $\mathbf{A}$, one can show that the eigenvalues are of the form $\lambda = \pm(r_1)^{1/2}, \pm(r_2)^{1/2}, \pm(r_3)^{1/2}$ and that the r's are distinct and are real numbers for $\omega > 0$. When $\lambda_i = +(r_i)^{1/2}$ for $i = 1, 2, 3$, the $a_j(l)$'s can be written in the following form:

$$a_0(l) = \frac{r_3 r_2 \cosh\lambda_1 l}{(r_3 - r_1)(r_2 - r_1)} - \frac{r_1 r_3 \cosh\lambda_2 l}{(r_3 - r_2)(r_2 - r_1)} + \frac{r_1 r_2 \cosh\lambda_3 l}{(r_3 - r_2)(r_3 - r_1)}$$

$$a_2(l) = \frac{(r_3 + r_2)\cosh\lambda_1 l}{(r_3 - r_1)(r_2 - r_1)} + \frac{(r_3 + r_1)\cosh\lambda_2 l}{(r_3 - r_2)(r_2 - r_1)} - \frac{(r_2 + r_1)\cosh\lambda_3 l}{(r_3 - r_2)(r_3 - r_1)} \tag{A5}$$

$$a_4(l) = \frac{\cosh\lambda_1 l}{(r_3 - r_1)(r_2 - r_1)} - \frac{\cosh\lambda_2 l}{(r_3 - r_2)(r_2 - r_1)} + \frac{\cosh\lambda_3 l}{(r_3 - r_2)(r_3 - r_1)}$$

$a_1(l)$, $a_3(l)$, and $a_5(l)$ are obtained by the relationships

$$a_i = a_i\,(\cosh\lambda l),\ a_{i+1} = (\sinh\lambda l/\lambda),\ i = 0, 2, 4 \tag{A6}$$

Note that even though r_i may be a negative number such that λ_i is a pure imaginary number, the $a_j(l)$'s remain real valued. Two limiting cases of the previous solution for $\mathbf{F}(l)$ are listed in Ref. 9.

The point transfer matrix for an elastic support with an attached stringer-link damping device, a link damper, and a tunnel damper at the same point as given by

$$\begin{bmatrix} 0 & 1 & 0 & 0 & 0 & 0 \\ 0 & 0 & 0 & 0 & 0 & 0 \\ 0 & 0 & 1 & 0 & 0 & 0 \\ a & 0 & \mu_1 & 1 & 0 & 0 \\ 0 & \mu_2 & 0 & 0 & 1 & 0 \\ \mu_3 & 0 & a & 0 & 0 & 1 \end{bmatrix} \tag{A7}$$

$u_1 = k_1 + b$
$\mu_2 = -k_2 - c + c' + c''$
$\mu_3 = k_3 + d$
k_1 = rotational spring stiffness
k_2 = radial deflection spring stiffness
k_3 = circumferential spring stiffness
$k_4 = k_{4d}(1 + ig_4)$ complex stiffness of stringer-link damper
$k_5 = k_{5d}(1 + ig_5)$ complex stiffness of link damper
$k_6 = k_{6d}(1 + ig_6)$ complex stiffness of tuned damper link
M = tuning mass of tuned damper
$a = l_0 k_4 \cos\phi$
$b = l_0^2 k_4 \cos\phi$
$c' = k_{5d}\,(1 + ig_5)$
$\omega_\tau^2 = k_{6d}/M$
$c = k_4 \sin\phi$

$$d = k_4 \cos\phi$$

$$c'' = \frac{\omega^2 k_{6d}/\omega_\tau^2}{1 - \omega^2/\omega_\tau^2(1 + ig_6)}$$

l_0 and ϕ are defined by Fig. 1. Any particular element can be removed from the point transfer matrix by setting the appropriate stiffness to zero.

References

[1] Miles, J. W., "Vibrations of Beams on Many Supports," *Journal of the Engineering Mechanics Division, American Society of Civil Engineers*, Vol. 82, No. EM1, Jan. 1956, pp. 1–9.

[2] Lin, Y. K., "Free Vibrations of a Continuous Beam of Elastic Supports," *International Journal of Mechanical Sciences*, Vol. 4, No. 5, Sept.–Oct. 1962, pp. 409–423.

[3] Wah, T., "Natural Frequencies of Uniform Grillages," *Journal of Applied Mechanics*, Vol. 30, No. 4, Dec. 1963, pp. 571–578.

[4] Lin, Y. K., Brown, I. D., and Deutschle, P. C., "Free Vibrations of a Finite Row of Continuous Skin-Stringer Panels," *Journal of Sound and Vibration*, Vol. 1, No. 1, Jan. 1964, pp. 14–27.

[5] Wah, T., "Flexural Vibrations of Ring-Stiffened Cylindrical Shells," *Journal of Sound and Vibration*, Vol. 3, May 1966, pp. 242–251.

[6] Lin, Y. K., "Free Vibration of Continuous Skin-Stringer Panels," *Journal of Applied Mechanics*, Vol. 27, No. 4, Dec. 1960, pp. 669–676.

[7] Schnell, W. and Heinrichsbauer, F., "Zur Bestimmung Der Eigenschwingungen Langsversteifter, Dunnwandiger Kreiszylinderschalen," *Jahrbuch der Wissenschaftliche Gesellschaft für Luft und Raumfahrt*, 1963, pp. 278–286.

[8] Lin, Y. K. and McDaniel, T. J., "Dynamics of Beam-Type Periodic Structures," *Journal of Engineering for Industry*, Vol. 91, No. 4, Nov. 1969, pp. 1133–1141.

[9] Pestel, E. C. and Leckie, F. A., *Matrix Methods in Elastomechanics*, McGraw-Hill, New York, 1963.

[10] Lin, Y. K. and McDaniel, T. J., "Response of Multi-Spanned Beam and Panel Systems under Noise Excitation," AFML-TR-64-348, Part II, Sept. 1967, Air Force Materials Lab., Wright-Patterson Air Force Base, Ohio.

[11] Clarkson, B. L. and Cicci, F., "Methods of Reducing the Response of Integrally Stiffened Structures to Random Pressures," *Journal of Engineering for Industry*, Vol. 91, No. 4, Nov. 1969, pp. 1203–1209.

[12] Jones, D. I. G., Henderson, J. P., and Bruns, G. H., "Use of Tuned Viscoelastic Dampers for Reduction of Vibrations in Aerospace Structures," *Proceedings of the 13th Annual Air Force Symposium*, Air Force Systems Command, Arnold Air Force Station, Tenn., Vol. 1, Paper 18, 1966.

[13] Schrumpich, G., "Beitrag zur Kinetik and Statik ebener Stabwerke mit gekrummten Staben," *Osterreichisches Ingenier-Archiv*, Vol. 11, 1957, pp. 194–225.

[14] Lin, Y. K. et al., "Free Vibration of Continuous Skin-Stringer Panels with Non-uniform Stringer Spacing and Panel Thickness," AFML-TR-64-348, Part I, Feb. 1965, Air Force Materials Lab., Wright-Patterson Air Force Base, Ohio.

[15] Doi, K. and Lin, Y. K., "Spatial Decay in the Response of Damped Periodic Structures," AFML-TR-69-308, Nov. 1969, Air Force Materials Lab., Wright-Patterson Air Force Base, Ohio.

MARCH 1971 J. AIRCRAFT VOL. 8, NO. 3

Dynamic Analysis of Stiffened Panel Structures

R. N. YURKOVICH*
McDonnell Douglas Corporation, St. Louis, Mo.

AND

J. H. SCHMIDT† AND A. R. ZAK‡
University of Illinois, Urbana, Ill.

The dynamic behavior of stiffened flat panels is analyzed using the method of finite-elements. The panels are stiffened by one or two sets of stiffeners which divide the panel into rectangular bays simulating a typical aircraft skin-frame-stringer configuration. The analysis is designed to investigate the free and the forced vibration behavior. In the case of the forced vibration, both undamped and damped response is examined where the damping is provided by viscoelastic dampers attached to the surface of the panel. The finite-element method consists of representing the panel by triangular plate elements, and the stiffeners are represented by beam elements which allow for bending, torsional, and warping effects. The latter effect is found to be very important. Examples are given, illustrating the application of the analysis to free and forced vibration problems. In the case of the latter, the effect of viscoelastic damping is examined and compared with experimental data. This data were obtained from an experimental investigation that was carried out in support of the theoretical analysis.

Nomenclature

A = matrix defined in Eq. (2)
A_1–A_9 = nine unknown coefficients in Eq. (1)
B = matrix defined in Eq. (8)
B_1–B_8 = eight coefficients in Eqs. (15) and (16)
C = matrix defined in Eq. (21)
C_{ws} = warping constant
D',D'' = real and imaginary parts of matrix defined in Eq. (32)
E = Young's modulus

Received February 24, 1970; revision received August 14, 1970. This work was sponsored by the Air Force Materials Laboratory, Air Force Systems Command under contract Number F33615-67-C-1190 at the University of Illinois.

* Structural Engineer. Associate Member AIAA.
† Graduate Student, Aeronautical and Astronautical Engineering Department. Member AIAA.
‡ Professor, Aeronautical and Astronautical Engineering Department. Member AIAA.